JOURNAL OF MATERIALS SCIENCE 24 (1989) 1683–1686

Estimation of the drawing efficiency of hot spinning of co-polyester fibres in producing high degrees of preferred orientation

J. C. JENKINS
Jenkins Instruments Ltd, The Innovation Centre, University College Swansea, Singleton Park, Swansea, SA2 8PP, UK

A range of liquid crystalline polyester fibres varying in diameter from 65 to 440 μm were produced by spinning from a hot melt. These were analysed for preferred orientation by flat-plate X-ray diffraction to produce equatorial azimuthal densitometry scans $I(\gamma)$ which were processed to produce the corresponding planar orientation profiles $I(\phi)$ corresponding to a Bragg separation of 0.448 nm. A further mathematical analysis was applied to these to produce the respective molecular orientation profiles $I(\alpha)$ which may be more directly related to fibre mechanical properties. $I(\alpha)$ profiles from this analysis were matched against theoretical $I(\alpha)$ calculated by assuming an idealized mechanism of affine deformation with no orientation losses due to thermal perturbations. The theoretical draws ratios corresponding to the experimentally observed $\langle\cos^2\alpha\rangle$ were matched against experimentally observed draw ratios to produce ratios which indicate drawing efficiencies. Although preferred orientation increased with increasing draw ratios, the drawing efficiency diminished with draw ratio.

1. Introduction

The analysis of the preferred orientation of the long molecules in polymer fibres is important in explaining their resulting anisotropic mechanical and physical properties. In liquid crystalline co-polyesters, the molecules are of a semi-rigid nature with strong intermolecular cohesion. This, combined with the induction of the large amounts of preferred orientation produced by fibre spinning, produces very stiff fibres. Co-polyesters have been spun either from solution [1, 2] or from the pure melt [2–4].

The rigorous characterization of the preferred orientation of the molecules involves analysis of the flat-plate X-ray meridional wide-angle reflections from molecular planes whose planar normals are orientated in the c-axis direction, or from equatorial wide-angle X-ray reflections whose planar normals are orientated at right angles to the c-axis. Where both types appear on an X-ray plate, the meridional reflections appear much weaker but slightly sharper.

The azimuthal analysis of the meridional reflections provides the more comprehensive description of low amounts of molecular preferred orientation in that the azimuthal X-ray intensity distribution around the X-ray plate $I(\gamma)$ may be more directly related to the molecular orientational distribution $I(\alpha)$ where α is the orientation angle between the normal of the diffracting meridional plane and the fibre direction.

$I(\alpha)$ is constructed from $I(\gamma)$ using the relation $\cos\gamma\cos\theta_B = \cos\alpha$ (where θ_B is the Bragg angle) for a fibre mounted upright in the X-ray beam. The orientation parameter $\langle\cos^2\alpha\rangle$ may then be calculated according to

$$\langle\cos^2\alpha\rangle = \frac{\int_0^{\pi/2} I(\alpha)\cos^2\alpha\sin\alpha\,d\alpha}{\int_0^{\pi/2} I(\alpha)\sin\alpha\,d\alpha} \quad (1)$$

for fibres with radial symmetry around their fibre axes.

However, meridional analysis has two disadvantages. Firstly, in cases of very high molecular orientation, the azimuthal X-ray intensity profile $I(\gamma)$ is masked by the convoluted X-ray intensity distribution of broadening due to strain and polycrystallinity. Secondly, meridional reflections are generally weak or non-existent in many of the X-ray patterns of fibre polymers in general. Equatorial reflections, on the other hand, are much stronger, enabling a well-defined equatorial planar orientational profile $I(\phi)$ to be constructed from $I(\gamma)$, the equatorial azimuthal intensity distribution. If ϕ is the angle between the normal of the planes in which the molecules lie and the fibre direction, then $I(\phi)$ may be constructed from equatorial $I(\gamma)$ using the relation $\cos\gamma\cos\theta_B = \cos\phi$.

In this work, a mathematical analysis based on work by Hermans *et al.* [5], Seitsonen [6, 7] and Biangardi [8] is applied which enables the molecular orientation functions $I(\alpha)$ of fibres to be constructed from $I(\phi)$ profiles of a liquid crystal co-polyester whose meridional reflections are too weak for objective analysis. $I(\alpha)$ profiles devised by numerical analysis for each fibre is matched against their theoretical counterparts derived from the experimental draw ratio assuming affine deformation of the molecules during fibre spinning [9].

0022–2461/89 $03.00 + .12

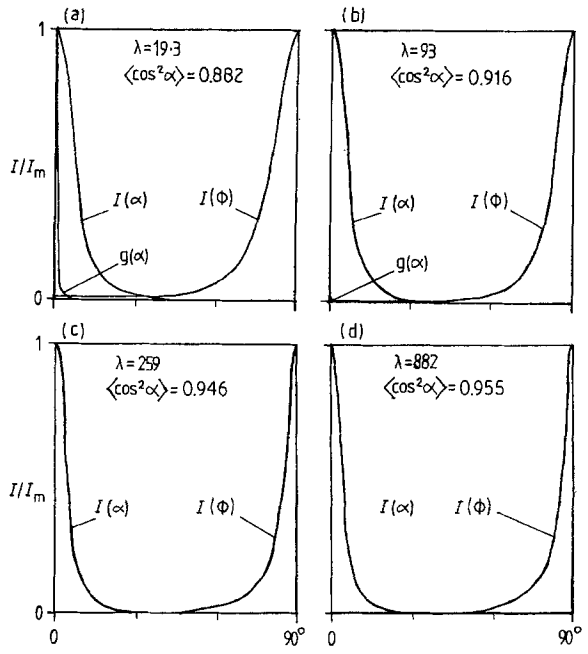

Figure 1 Equatorial planar orientation distributions $I(\phi)$ and the derived molecular orientation distributions $I(\alpha)$ for fibres of diameter (a) 440 μm, (b) 200 μm, (c) 120 μm, and (d) 65 μm. I_m is the respective maximum intensity.

Other workers [10, 11] have extensively analysed equatorial and meridional X-ray diffraction traces to characterize the intrinsic nature of the preferred orientation of liquid crystalline polyester fibres in terms of both local and bulk distributions. This work, however, does not attempt to characterize these, but rather attempts to relate the normally described preferred $I(\alpha)$ orientation in terms of the efficiency of the hot drawing process in producing high amounts of preferred orientation. Preliminary work on three of the four fibres examined has already been reported [12] relating stiffnesses to preferred orientation, but does not include the mathematical deduction of the equatorial planar and molecular orientation distributions which follow.

2. Experimental procedure

Fibres of 65, 120, 200 and 440 μm were produced by hot spinning from a 300° C melt by a process described previously [12], the 65 μm fibre being the new addition. After flat-plate X-ray diffraction (with the specimens mounted upright in the X-ray beam) and densitometry to produce $I(\gamma)$ from the strong equatorial 0.448 nm reflections, the respective equatorial planar orientations $I(\phi)$ were deduced using the cos ϕ relation referred to in the Introduction.

Fig. 1 depicts the orientation functions of the four fibres with $\phi = 90°$ corresponding to the fibre axes. Strictly speaking, it is only possible to deduce $I(\phi)$ between ϕ equal to 90° and arc cos (cos γ cos θ_B) = 9.9°, but for fibres of high orientation, the missing range between ϕ equal to 9.9° and 0° may be deduced by extrapolation because $I(\phi)$ tends to flatten out at low values of ϕ.

The construction of the molecular orientation functions $I(\alpha)$ and their theoretical counterparts $g(\alpha)$ for each draw ratio, also shown in Fig. 1, is discussed below.

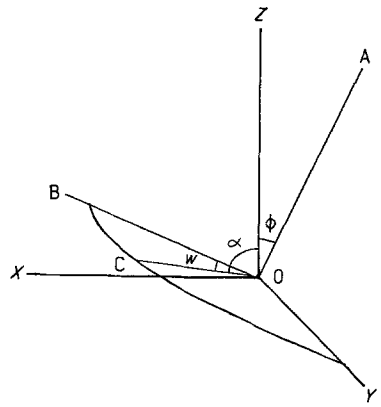

Figure 2 The relationship between molecular intensity $I(\alpha)$ depicted by line OC and planar intensity $I(\phi)$ obtained by integrating all $I(\alpha)$ values in the quadrant BOY, where OZ is the fibre direction.

3. Discussion

Fig. 2 shows how a set of molecular segments, lying in a plane whose normal is orientated at ϕ to fibre axes, range in molecular orientation from $\alpha = (\pi/2) - \phi$ to $\alpha = \pi/2$, corresponding to lines OB and OY in Fig. 2, respectively. Assuming radial symmetry, only at $\phi = 0$ can $I(\phi)$ consist of molecules of one value of α, i.e. $\alpha = \pi/2$ corresponding to line OZ. In this case, $I(\phi = 0)$ is equivalent to $I(\alpha = 0)$.

Integrating the molecular segment intensities $I(\alpha)$ in the quadrant BOY between $w = 0$ and $\pi/2$ gives the corresponding planar intensity $I(\phi)$ for any planar normal position at ϕ generated about OZ, i.e.

$$I(\phi) = \int_0^{\pi/2} I(\alpha)\, dw = \int_{\pi/2-\phi}^{\pi/2} I(\alpha) \frac{dw}{d\alpha} d\alpha \quad (2)$$

where

$$w = \arccos(\cos\alpha \operatorname{cosec}\phi) \quad (3)$$

Thus

$$I(\phi) = \int_{\pi/2-\phi}^{\pi/2} \frac{I(\alpha)\sin\alpha\, d\alpha}{(\sin^2\phi - \cos^2\alpha)^{.5}} \quad (4)$$

This equation is similar to that derived by Hermans *et al.* [5], but the analysis from hereon differs from that first presented by Seitsonen [6] for the solution of $I(\alpha)$ from values of $I(\phi)$.

The equation representing the numerical solution of Equation 2 for each $I(\alpha)$ is

$$I(\phi_m) = I(\alpha_1)\Delta w_1 + I(\alpha_2)\Delta w_2 + \ldots + I(\alpha_n)\Delta w_m \quad (5)$$

where

$$\alpha_1 = (\pi/2) - \tfrac{1}{2}\Delta\alpha \quad (6)$$

and

$$\alpha_n = (\pi/2) - \Delta\alpha\,(n + \tfrac{1}{2}) \quad (7)$$

where

$$1 \leqslant n \leqslant m \quad (8)$$

and

$$\Delta\alpha = \alpha_n - \alpha_{n+1} \quad (9)$$

TABLE I Thermal expansion data for isotropic (a_i) and oriented specimens ($a_\perp$) at 150° C

$a_\perp$ (K^{-1})	1.67×10^{-4}
a_i (K^{-1})	0.91×10^{-4}

With respect to Equation 3

$$\Delta w_n = \arccos[\cos(\alpha_n + \tfrac{1}{2}\Delta\alpha)\operatorname{cosec}\phi_m) - \arccos[\cos(\alpha_n - \tfrac{1}{2}\Delta\alpha)\operatorname{cosec}\phi_m] \quad (10)$$

The value of each $I(\alpha)$ may be calculated in turn, starting with $I(\alpha_1)$ where $\alpha_1 = (\pi/2) - \frac{1}{2}\Delta\alpha$ at the low orientation end being assumed equivalent to $I(\phi_1)$ where $\phi_1 = \Delta\alpha$. In this case, $\Delta w_1 = \pi/2$ and Equation 5 becomes

$$I(\phi_1) = (\pi/2)I(\alpha_1) \quad (11)$$

where $\phi_1 = 0°$ and $\alpha_1 = 90°$.

Knowing $I(\alpha_1)$ and the planar intensity $I(\phi_2)$ at $\phi_2 = 2\Delta\alpha$, $I(\alpha_2)$ may be solved from Equation 5 by

$$I(\phi_2) = I(\alpha_1)\Delta w_1 + I(\alpha_2)\Delta w_2 \quad (12)$$

If, for example, measurements of $I(\phi)$ were made in intervals of 1° as was employed in this work, implying $\Delta\alpha = 1°$, Equation 12 would be solved for $I(\alpha_2 = 88.5°)$ by

$$I(\phi_2 = 2°) = I(\alpha = 89.5°)[(\arccos(\cos 90° \operatorname{cosec} 2°) - \arccos(\cos 89° \operatorname{cosec} 2°)] + I(\alpha = 88.5°)[\arccos(\cos 89° \operatorname{cosec} 2°) - \arccos(\cos 88° \operatorname{cosec} 2°)] \quad (13)$$

$I(\alpha = 89.5°)$ may be estimated as $I(\alpha = 90°)$ because $dI(\alpha)/d\alpha \to 0$ as $\alpha \to 90°$ in Fig. 1.

Knowing $I(\alpha_1)$ and $I(\alpha_2)$, $I(\alpha_3)$ may be solved from Equation 5 by

$$I(\phi_3 = 3°) = I(\alpha_1)\Delta w_1 + I(\alpha_2)\Delta w_2 + I(\alpha_3)\Delta w_3 \quad (14)$$

The normalized $I(\alpha)$ profiles for each of the four fibres may be compared with their corresponding $I(\phi)$ profiles in Fig. 1. $I(\alpha)$ is sharper than $I(\phi)$, especially for the first two fibres where $I(\alpha = 10°)$ is about half of $I(\phi = 80°)$. For each fibre, $I(\alpha)$ may also be compared with its theoretical counterpart $g(\alpha)$ derived from a knowledge of the draw ratio employed in the production of each fibre, assuming affine deformation first proposed by Kratky [9]. In this idealized model of draw-induced preferred orientation, each molecular segment at any initial orientation α_0 rotates to lie closer to the drawing direction with no loss of orientation due to thermal perturbations. Hence, the only factor predicting the final orientation function is the geometry of the drawing deformation, i.e. if λ is the draw ratio, then

$$\cot\alpha_1 = \lambda^{1.5}\cot\alpha_0 \quad (15)$$

and the final orientation function $g(\alpha)$ derived by Kratky, assuming an initial isotropic arrangement of molecules before drawing, is given by

$$g(\alpha) = \frac{1}{[\lambda^3 - (\lambda^3 - 1)\cos^2\alpha]^{1.5}} \quad (16)$$

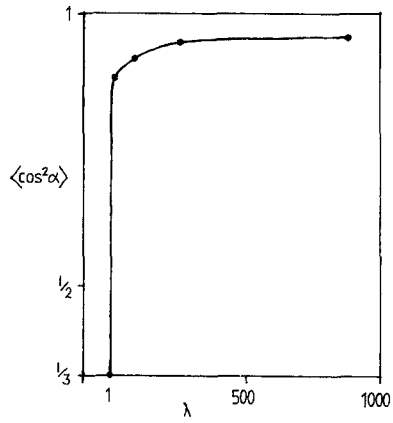

Figure 3 Experimental $\langle\cos^2\alpha\rangle$ for all four fibres related to draw ratio λ.

In order to calculate the true draw ratios for the final diameters of the four fibres, it is necessary to know the respective hot diameter (d_h) at the extrusion temperature so that the reduction in diameter due to thermal expansion is corrected for. The hot diameter, d_h, is calculated by $d_0(1 + a\Delta T)$ where d_0 is the cold diameter, and a is thermal expansion between ambient and the extrusion temperatures (ΔT). The true draw ratio is then calculated by d_0^2/d_h^2 where d_0 is the orifice diameter. Values of a may differ slightly due to differences in preferred orientation between fibres, but in each case it would lie between that corresponding to isotropy (a_i); and that corresponding to near-perfect preferred orientation perpendicular to the length of the molecules ($a_\perp$). Co-polyester prepared by hot pressing powder or very thin fibres together, to produce isotropic and anisotropic specimens, respectively, were measured for thermal expansion in a dilatometer at 150° C and the results are given in Table I.

The mean value of $1.29 \pm 0.38 \times 10^{-4} K^{-1}$ was thus used to estimate the hot diameter d_h for all fibres. The true draw ratios λ calculated by d_0^2/d_h^2 were employed to construct the theoretical orientation functions $g(\alpha)$ appearing in Fig. 1a for the thickest 440 μm fibre. $g(\alpha)$ for the 200 μm fibre is very sharp and only appears to deviate from $\alpha = 0$ right at the bottom. $g(\alpha)$ for the two thinnest fibres are so sharp that they cannot be represented in Figs 1c and d.

Values of $\langle\cos^2\alpha\rangle$ calculated from Equation 1 for

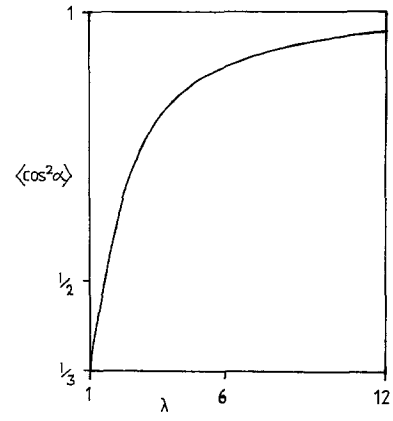

Figure 4 $\langle\cos^2\alpha\rangle$ calculated according to affine deformation related to draw ratio λ.

TABLE II Drawing efficiency (DE) of the co-polyester fibres

Diameter (μm)	$\langle\cos^2\alpha\rangle$	λ	λ_e	DE (%)
440	0.882	19.3	5.25	27.2
200	0.916	93	6.72	7.2
120	0.946	259	9.18	3.5
65	0.955	882	10.4	1.2

the experimental $I(\alpha)$ are plotted against draw ratio, λ, in Fig. 3. The point at $\lambda = 1$ corresponds with the assumption of isotropy before drawing with $\langle\cos^2\alpha\rangle = 1/3$. It is seen that after spinning past a draw ratio of 300, very little gain is made in preferred orientation with $\langle\cos^2\alpha\rangle$ tending to level out at about 0.955. Fig. 4 also shows values of $\langle\cos^2\alpha\rangle$ against draw ratio λ, this time calculated by replacing $I(\alpha)$ with the idealized $g(\alpha)$ of Equation 16 in Equation 1. Hence, comparisons of the actual extents of draw-induced preferred orientation in Fig. 3 may be made against those assuming affine deformation. For example, Fig. 3 shows that a $\langle\cos^2\alpha\rangle$ of 0.95, which is typical of fine fibres in general, is produced by a draw ratio of about 300 in the co-polyester, whereas Fig. 4 shows that consideration of the geometry of deformation alone would predict an equivalent draw ratio (λ_e) of 9.7 to produce the same extent of orientation.

The ratio of these two draw ratios provides a useful parameter which directly expresses the efficiency of hot drawing at a particular stage during drawing. If this was expressed as a percentage in the case above, the drawing efficiency would be 3.2% for a draw ratio of 300. Table II shows the drawing efficiency of all four fibres, indicating a fall off with increasing draw ratio.

4. Conclusions

The above analysis shows that increasing the draw ratio of liquid crystal polyester produces an increasing deviation from a mechanism of deformation predicted by geometric considerations alone. Affine deformation involves a mixture of rotational and translational movement of the semi-rigid molecules during idealized drawing with the rotational component only contributing to the enhancement in preferred orientation. The results show that ever-greater proportions of translational molecular motion, over and above that expected in pure affine deformation, are involved in drawing at higher draw ratios.

Previous work on the same material has shown that the Young's modulus increases from approximately 32 to 60 GPa as the fibre diameter decreases from 440 to 60 μm [12], thus demonstrating the importance of maximizing the preferred orientation. Annealing is usefully employed in enhancing the mechanical properties of fibres in general, in that both crystallinity and preferred orientation are improved when the optimum heat-treatment temperature is employed. Therefore, the preceeding analysis of equatorial diffraction traces may be applied not only to characterize drawing efficiency, but also changes in preferred orientation on further heat treatment.

Acknowledgements

The author thanks Dr G. M. Jenkins for some interesting comments on the work, I. C. I. Wilton, for the supply of the co-polyester, K. Saib for assistance in fibre preparation, and SERC Daresbury Laboratories, for densitometry of the X-ray data.

References

1. D. C. PREVORSEK, in "Polymer Liquid Crystals", edited by A. Ciferri, W. Krigbaum and B. Meyer (Academic, New York, 1982) Ch. 12.
2. A. CIFERRI and B. VALENTI, in "Ultra High Modulus Polymers", edited by A. Ciferri and I. M. Ward (Applied Science, London, 1979) Ch. 7.
3. D. ACIERNO, F. R. LA MARTIA, G. POLIZZOTTI, A. CIFERRI and B. VALENTI, *Macromolec.* **15** (1982) 1455.
4. K. SHIMAMURA, J. L. WHITE and J. F. FELLES, *J. Appl. Polym. Sci.* **26** (1981) 2165.
5. J. J. HERMANS, D. H. HERMANS, D. VERMAAS and A. WEIDINGER, *Rec. Trav. Chim. Pays-Bas* **65** (1946) 427.
6. S. SEITSONEN, *J. Appl. Crystallogr.* **1** (1968) 82.
7. *Idem, ibid.* **6** (1973) 44.
8. H. J. BIANGARDI, *J. Polym. Sci.* **8** (1980) 903.
9. O. KRATKY, *Kolloid. Zh.* **64** (1933) 82.
10. G. R. MITCHELL and A. H. WINDLE, *Polymer* **24** (1983) 1513.
11. A. BISURAS and J. BLACKWELL, *Macromolec.* **20** (1987) 2997.
12. J. C. JENKINS and G. M. JENKINS, *J. Mater. Sci.* **22** (1987) 3784.

Received 14 April
and accepted 7 September 1988